ALGORITHMS FOR ON-LINE

PARAMETER AND MODE SHAPE ESTIMATION

Frederick E. Thau
The City University of New York
New York, N.Y.

One of the schemes that has been proposed for the adaptive control of large flexible space structures is shown in figure 1. This approach is based upon a modal decomposition of the dynamic response of the flexible structure and is designed to make use of the parallel processing features of modern minicomputers. Satisfactory performance of the parallel structure identification technique shown in figure 1 can be achieved only when the approximation functions noted in the figure correspond to the natural modes of the flexible structure. The work summarized here presents a technique for estimating both mode shapes and modal parameters.

$$w(s,t) = \sum_{i=1}^{NM} q_i(t, p_i)\, \epsilon_i(s) + \sqrt{}(s,t)$$

(a) Motion of flexible structure.

$$q(k+1) = A_1 q(k) + A_2 q(k-1) + B_1 U(k) + B_2 U(k-1)$$

$$y(k) = H_q(k) + w(k)$$

(b) Modal description.

Figure 1.- Problem formulation.

Figure 2 shows the analytic background for the formulation of the on-line identification problem. The motion of the flexible structure is expressed as a sum of NM terms involving the modal shape function $\xi_i(s)$ and the modal amplitudes $q_i(t,p_i)$ where s denotes the spatial variable and t represents time. The parameter vector p_i represents a set of parameters $[A_{1i},A_{2i},\tilde{B}_{1i},\tilde{B}_{2i}]$ for each mode. The identification problem is formulated in terms of the modal description shown in figure 2(b), where the $A_i, i=1,2$ are diagonal matrices of order NM, U(k) denotes a vector of actuator signals and the B_i are rectangular matrices. Matrix H, relating the modal amplitudes to the measurement vector y(k), has columns that are linearly independent in the modal model. On-line measurements $\{y(k)\},\{U(k)\}$ are to be processed in order to obtain estimates of the matrices A_i, B_i, and H.

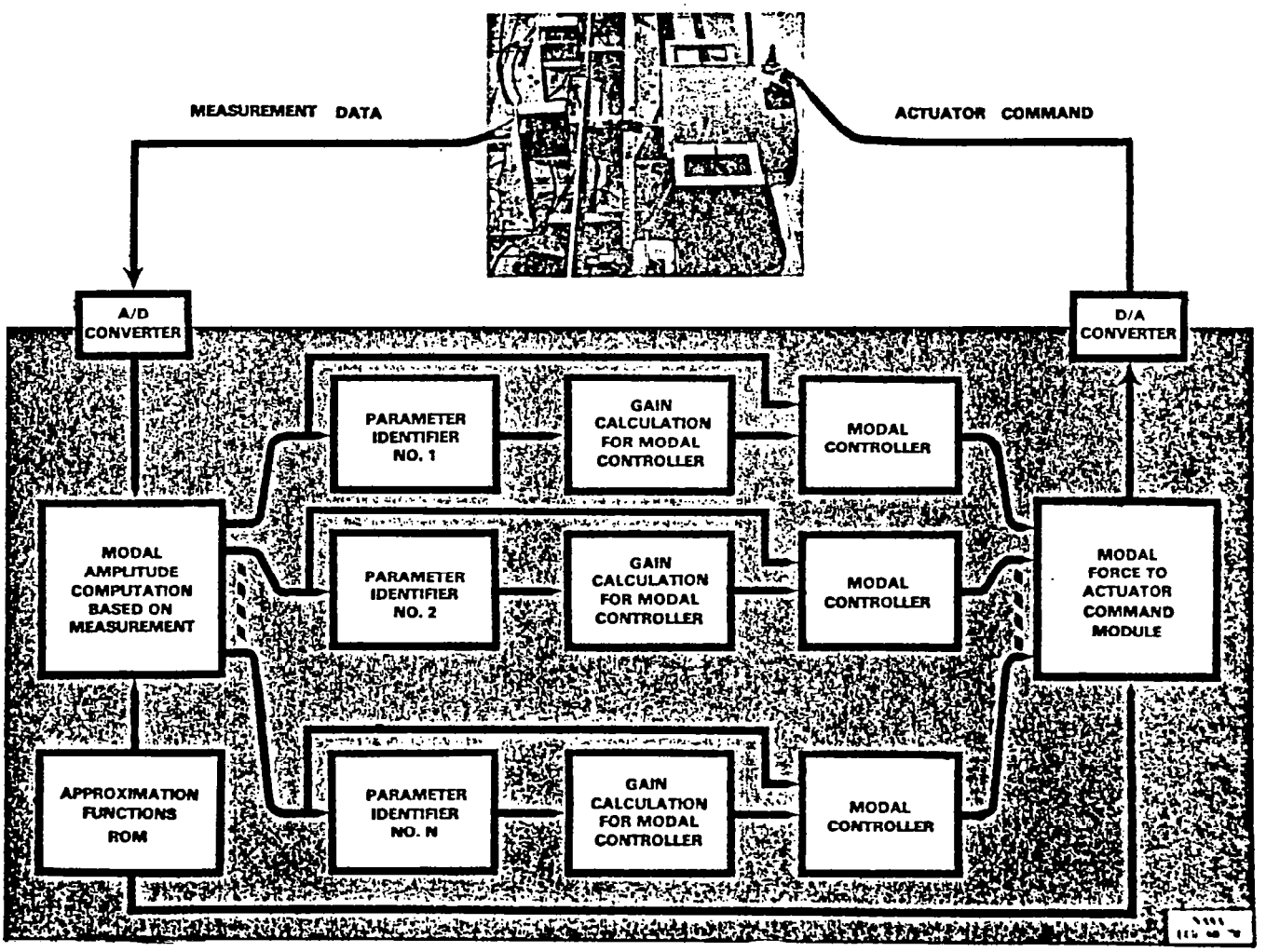

Figure 2.- Distributed adaptive control.

Algorithms for on-line parameter identification are shown in figure 3. Assuming that the approximation functions are given, the modal parameters are updated using an output error formulation where the error e_i is given by

$$e_i(k-1) = q_i(k-1) - A_{1i}q_i(k-2) - A_{2i}q_i(k-3) - \tilde{B}_{1i}F_i(k-2) - \tilde{B}_{2i}F_i(k-3)$$

where $F_i(k)$ denotes a modal force component. The weights W_i are selected to satisfy

$$W_1q_i^2(k-2) + W_2q_i^2(k-3) + W_3F_i^2(k-2) + W_4F_i^2(k-3) < 2$$

to insure stability of the identification algorithm.

The approach for updating the approximation functions is based on combining the modal equations shown in figure 2 into the single relation involving matrices M_i and N_i where

$$M_i = HA_iH^+ \qquad i = 1,2$$
$$N_i = HB_i$$

and $(H)^+$ denotes the pseudo-inverse of H. Using a regression analysis approach, data are collected over a time interval of length N and a least-squares estimate of M_i and N_i is obtained. When the number of modes in the modal approximation is the same as the number of sensors, the eigenvectors of M_i correspond to the columns of H.

$$p_i(k) = p_i(k-1) + e_i(k-1)\cdot\begin{bmatrix} W_1q_i(k-2) \\ W_2q_i(k-3) \\ W_3F_i(k-2) \\ W_4F_i(k-3) \end{bmatrix}$$

(a) Pole-zero characteristics - output error formulation.

$$y(k+1) = M_1y(k) + M_2y(k-1) + N_1U(k) + N_2U(k-1) + n(k+1)$$

$$N \updownarrow Y(N) = S(N)M^T + V(N);\quad M^T = \begin{bmatrix} M_1^T \\ M_2^T \\ N_1^T \\ N_2^T \end{bmatrix}$$

$$\hat{M}^T = S^+(N)Y(N)$$

(b) Approximation functions - regression analysis.

Figure 3.- On-line parameter identification.

A schematic diagram of the flexible beam used to test the identification algorithms is shown in figure 4. Sensor and actuator locations along the beam are shown along with the modal frequencies and mode shapes for the first three flexible modes obtained from the SPAR analysis program.

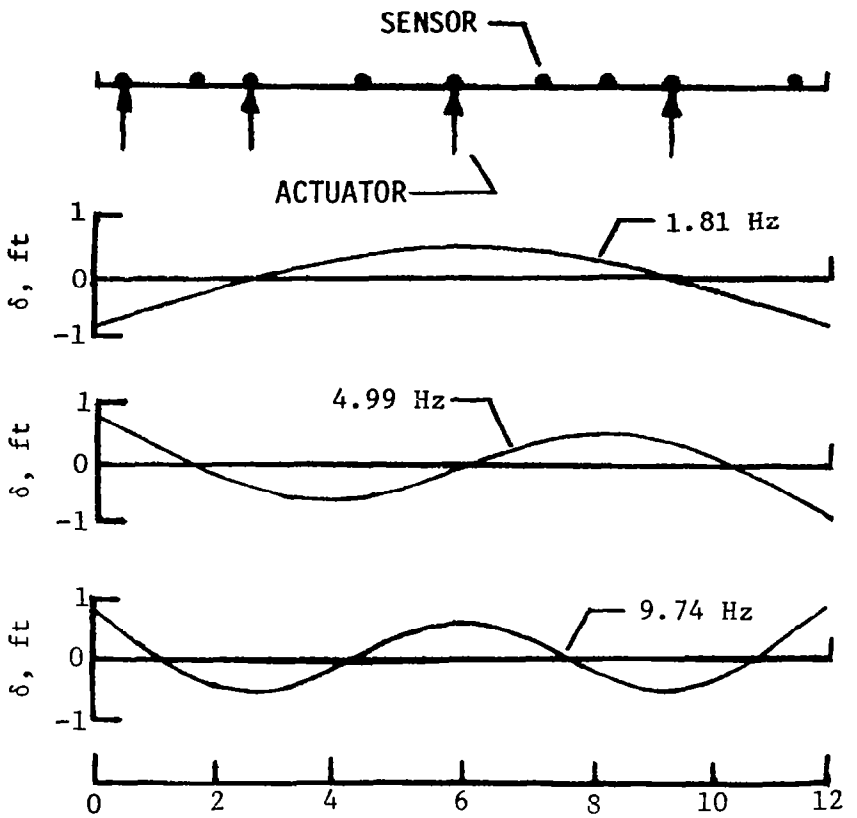

Figure 4.- Modes of interest.

Figure 5 shows the modal decomposition for mode 3 unforced response. A set of approximation functions obtained from the SPAR analysis was used and eight modes were assumed in the real-time program that produced the modal amplitude signals shown. For this response there is some excitation of modes 1 and 2. However, higher frequency modes do not appear to be excited.

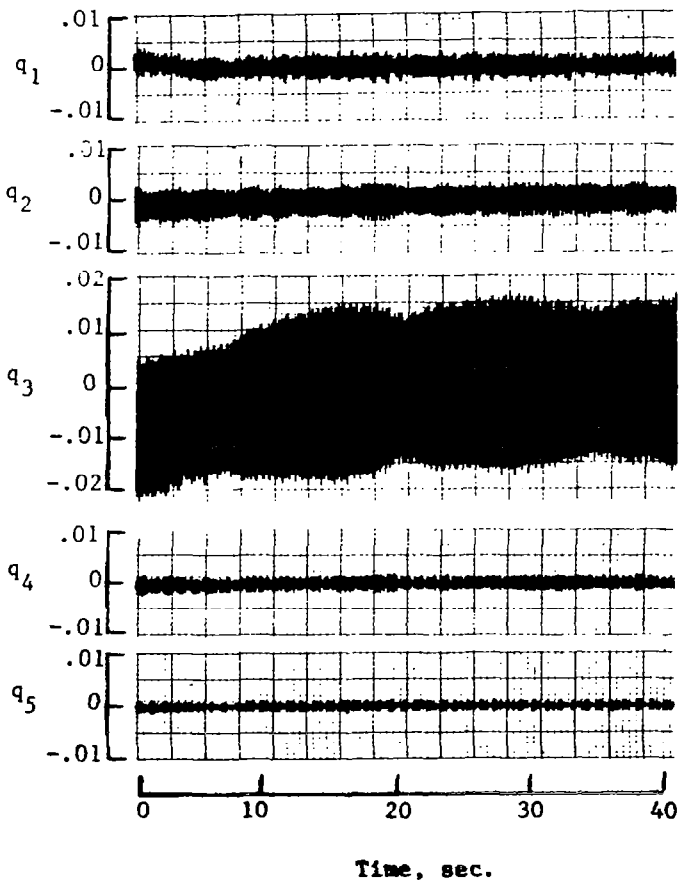

Figure 5.- Modal decomposition.

Eight SPAR modes; mode 3 excited.

Outputs of four on-line identifiers that result from self-sustained oscillation of the third vibration mode are shown in figure 6. Note that before the sustained oscillation occurs the identifiers are responding to measurement noise. Upon initiation of the sustained oscillation the parameters of the vibrating mode are rapidly identified. The parameters p_j^i correspond to the j^{th} diagonal element of the matrix A_i, $i = 1,2$, shown in figure 2. Also shown in the figure are the modal parameters derived from the structural analysis program.

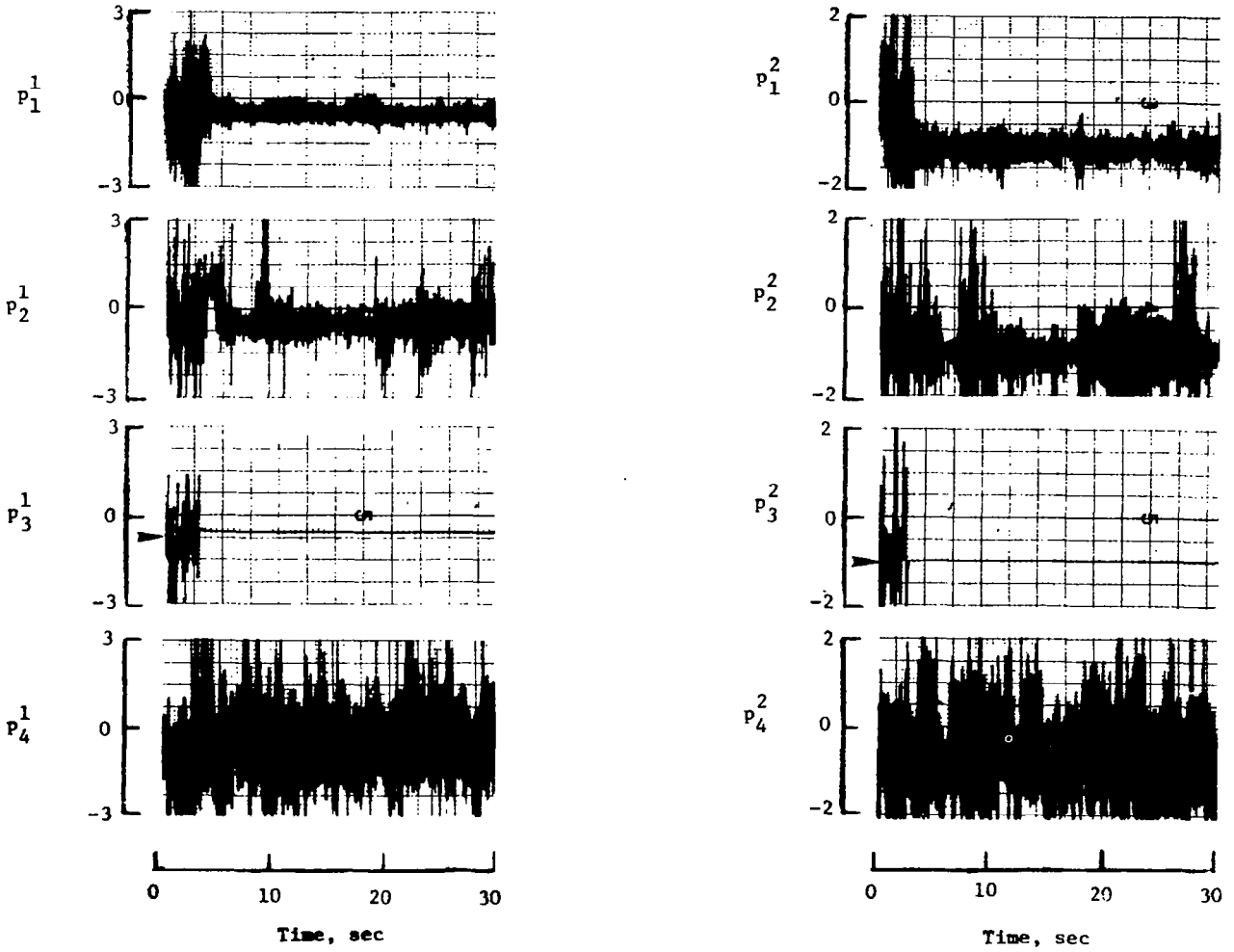

Figure 6.- Output of parameter identifiers. SPAR derived values; mode 3 excited.

Figure 7 shows the outputs of four on-line identifiers resulting from a 5-Hz excitation produced by actuator 1. Note that the parameters of the first vibration mode are identified but the high frequency modal parameters are not found as a result of the 5-Hz excitation.

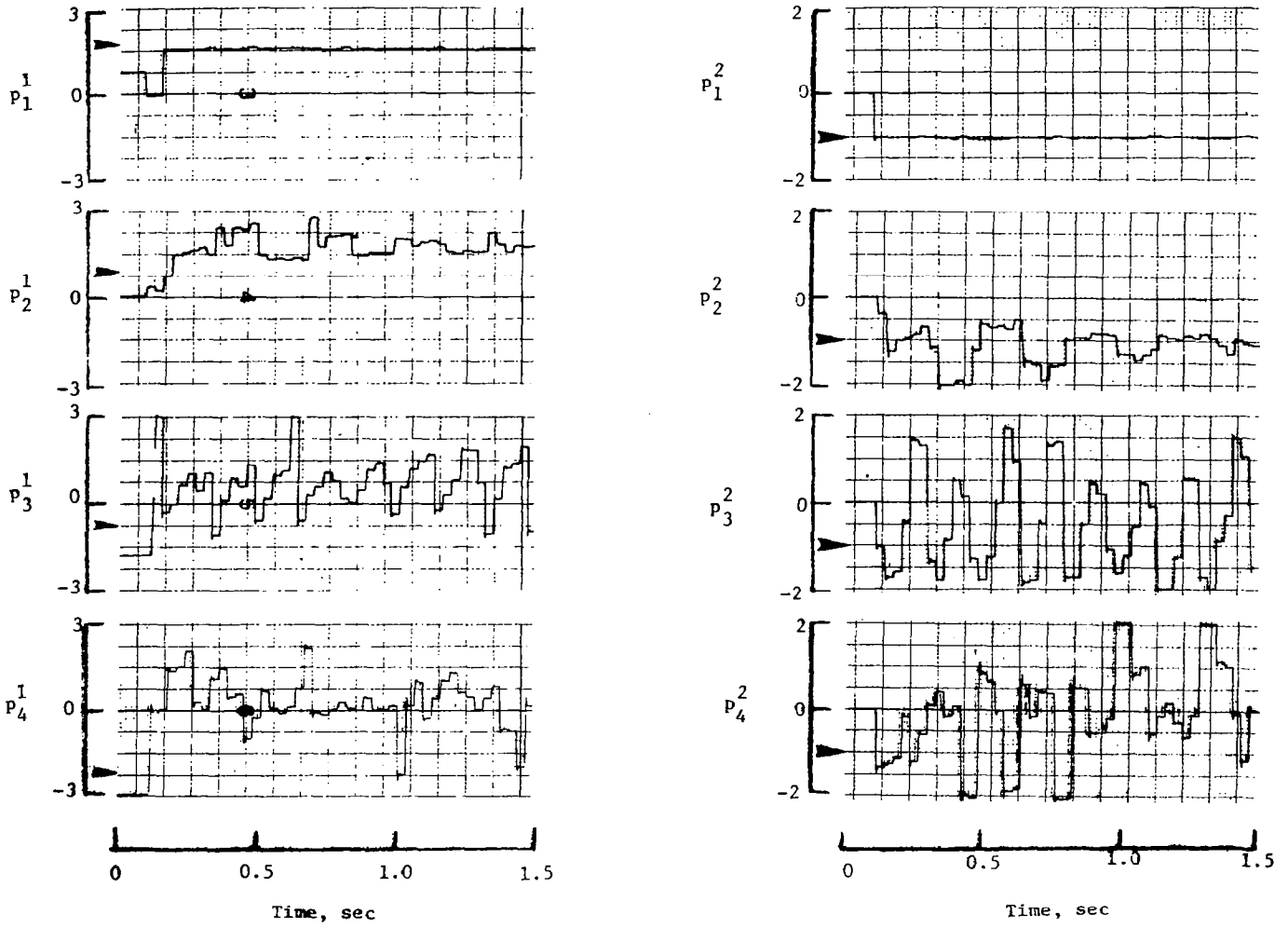

Figure 7.- Output of parameter identifiers. SPAR derived values. Sinusoidal excitation by actuator 1 at 5 Hz.

Figure 8 demonstrates the result of applying the mode shape identification procedure (a) to a simulation wherein the beam was given an arbitrary displacement and (b) in an experiment wherein only the first flexible mode was excited. In the simulation the normalized mode shape obtained agreed with that produced by the SPAR analysis. However, in the laboratory experiment a distortion in the identified mode shape was observed. In both cases the mode shape was identified on line after approximately 1 second of data processing.

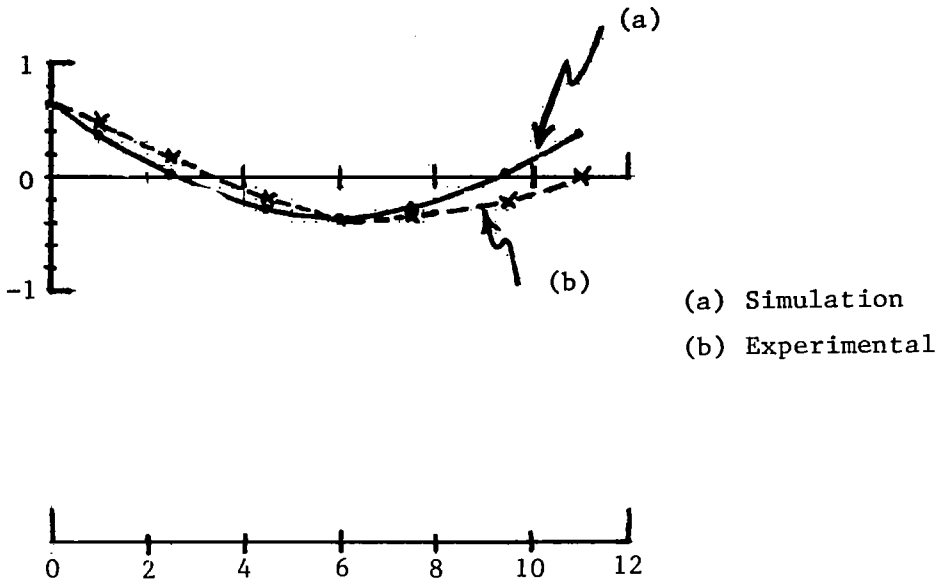

Figure 8.- Identification of mode shape.
First flexible mode.

A table of identified modal parameter values that resulted from a simulation incorporating both the mode shape and modal parameter identification schemes is shown in figure 9. Identification of mode shapes and parameters was accomplished in approximately 1 second of processing measurements from eight sensors distributed along the beam.

[Simulation - all modes excited at parameter values]

Flexible mode	Initial	Final	Actual
1	-0.8495	1.8726	1.87267
2	-1.7194	1.0991	1.099181
3	0.09918	-0.71936	-0.71940
4	0.83907	-1.9960	-1.9960
5	0.8726	0.15047	0.15049
6	-2.996	1.8387	1.83907

Figure 9.- Identification of modal parameters.

SUMMARY

- Presented algorithms for on-line parameter and mode-shape estimation
- Examined identification performance using computer simulations and a limited number of laboratory experiments
- Future work will include:

  (1) Further experimental studies

  (2) Development of separable nonlinear least-squares approach to identification

  (3) Development of on-line performance measures for sequential processing decisions